

R-Modes on Rapidly Rotating, Relativistic Stars : II. Blackbody Emission

Jeremy S. Heyl^{1,2}

ABSTRACT

Rossby waves (or r-modes) on the surface of a neutron star have become a leading model for the oscillations observed during the tail of Type-I X-ray bursts. Their frequency evolution matches well with the observed frequency drifts of the oscillations in the bursts, and the burning appears to excite these waves quite naturally. This paper addresses the detailed shape of the expected flux profiles from r-modes on neutron stars as a function of energy. R-modes naturally account for both the small amplitude of the observed oscillations and their lack of harmonic content. However, the model predicts that the oscillation at higher energies leads the lower energy variation. The observed oscillations have the opposite trend which possibly indicates that the higher energy photons are upscattered in the plasma surrounding the neutron star and therefore delayed.

1. Introduction

Heyl (2004) proposed that the oscillations in the tail of Type-I X-ray bursts are the signatures of Rossby waves travelling on the surface of the neutron star. This model predicts a specific pattern of hot and cold regions on the surface of the star. Ford (1999) proposed that spectral dependence of Type-I X-ray burst oscillations may provide an important probe of the mass and radius of neutron stars. Muno et al. (2002, 2003) examined the observed energy dependence and harmonic content of burst oscillations. Cadeau et al. (2005) have studied the propagation of radiation in the equatorial plane surrounding rotating neutron stars with realistic equations of state in a full general relativistic treatment with a hot-spot model for the emission. Leaving the equatorial plane in a general spacetime makes the treatment of photon propagation much more complicated.

This paper fills a gap in these various discussions. Specifically the emission from the surface of the star takes the form of a r-mode (Heyl 2004) that can account for the observed frequency shifts of Type-I x-ray burst oscillations from rapidly rotating neutron stars in low-mass x-ray binaries and combines this emission model with a general relativistic treatment of the photon propagation in a Kerr spacetime surrounding a rapidly rotating neutron star. This treatment is essentially valid to first order in the spin of the star Ω because it assumes a particular relationship between the

¹Chandra Fellow; Harvard-Smithsonian Center for Astrophysics, MS-51, 60 Garden Street, Cambridge MA 02138, United States

²Current Address: Department of Physics and Astronomy; University of British Columbia; Vancouver, BC V6T 1Z1, Canada; hey1@physics.ubc.ca

higher moments of the gravitational field that is not valid to second order. Furthermore, it neglects the distortion of the stellar surface due to rapid rotation. Neglecting the rotational perturbations to the metric at the beginning of § 4 yields an estimate of the error in the former approximation. Understanding latter approximation would require modelling the structure of the neutron star in full general relativity (e.g. Stergioulas & Friedman 1995). The main thrust of this paper is to confront theoretical predictions with observations, such as those of Muno et al. (2002, 2003), so this latter comparison is beyond the scope of this paper.

2. Calculational Overview

As Heyl (2004) assumed, the r-mode perturbs the local effective temperature of the emission by an amount proportional to the instantaneous amplitude of the mode at the location. Furthermore the emergent spectrum is taken to be a blackbody. However, unlike Heyl (2004), the calculation here will account for the rapid rotation of the star and examine the detailed shape of the light curves, not only the pulsed fraction. The rapid rotation affects the observed profiles in three ways.

First, the spacetime surrounding the star no longer is Schwarzschild. The exterior spacetime will be approximated by the Kerr geometry which assumes a particular ratio between the higher moments of the gravitational field. The distortion of the star due to the rapid rotation is not included. The results show that the perturbation to the geometry is not important at least for stars rotating up to 600 Hz. Cadeau et al. (2005) found that a Schwarzschild plus Doppler treatment (in which the moment of inertia vanishes) gives good results *vis a vis* a fully relativistic treatment. Second, the photons from different parts of the surface take different amounts of time to reach the observer. During this delay the star may rotate significantly. Third, there is a significant difference in the redshift from different regions of the stellar surface. To examine all of the these effects separately, the fully relativistic calculations will be contrasted with rapidly rotating stars with a vanishing moment of inertia and models where the time delay and redshift factors are separately neglected.

To determine what observations of the r-mode oscillation may reveal, several values for the strength of the r-mode and its frequency are studied. Also the radius and spin frequency of the star, and the line of sight of the observer are varied. Table 1 shows the various parameters and the values considered. Although this study considers only a single value for the stellar mass, results may be obtained for different masses by scaling the stellar radius with the mass and the spin frequency inversely with the mass. If one includes the models calculated with various physical effects neglected, the total number is 1200. The total flux and flux densities at five different energies are calculated as a function of phase to determine the pulsed fraction and harmonic content of the oscillations.

The next section presents the details of how the light curves are calculated (§ 3). A reader not interested in these details may be forgiven for skipping to § 4 that presents the results. § 5 relates

these results both to the observations and previous theoretical work.

3. Calculational Details

The calculation follows the techniques outlined in the appendix of Chen & Shaham (1989). Specifically, the photon paths begin at the observer and are evenly spaced over the image plane. Before integrating a particular path, the constants of the photon's motion are determined: its energy, $E = -P_t$, its specific angular momentum, $l = -P_\phi/P_t$ and its specific Carter constant $q = P_\theta^2/P_t^2 - a^2 \cos^2 \theta + l^2 \cot^2 \theta$. If the value of q is too small or l is outside a particular range, the photon will not reach the stellar surface, so its path is not integrated. Those paths for those photons that pass these criteria are integrated until either they reach the surface or they reach their minimum radius. If the ray intersects the surface, the redshift of the surface relative to infinity including the velocity of the surface element is calculated.

Chen & Shaham (1989) present the variables and metric in detail, but for clarity the key equations are

$$\frac{d\theta}{dr} = \pm \frac{(q - l^2 \cot^2 \theta + a^2 \cos^2 \theta)^{1/2}}{V_r^{1/2}} \quad (1)$$

$$\frac{d\phi}{dr} = \frac{-a + l \csc^2 \theta + a(r^2 + a^2 - la)/\Delta}{V_r^{1/2}} \quad (2)$$

$$\frac{dt}{dr} = \frac{D - 2Malr}{V_r^{1/2} \Delta} \quad (3)$$

where

$$\Delta = r^2 - 2Mr + a^2 \quad (4)$$

$$D = (r^2 + a^2)^2 - a^2 \Delta \sin^2 \theta \quad (5)$$

$$V_r = (r^2 + a^2 - la)^2 - \Delta(l^2 + a^2 - 2la + q). \quad (6)$$

These equations are expressed in units with $G = c = 1$. Asymptotically far from the star, r, θ and ϕ are the usual spherical coordinates and t is the time coordinate. a is the ratio of the angular momentum of the star to its mass. The results of Ravenhall & Pethick (1994) give $J = 0.21MR^2\Omega/(1 - 2GM/Rc^2)$ for slowly rotating neutron stars. For the models outlined in Table 1, a/M ranges from 0 to 0.721.

Because the integration begins at the detector and proceeds toward the star, the rays can be spaced equally in solid angle at infinity. Because the locally measured intensity divided by fourth power of the locally measured energy is a relativistic invariant along a ray bundle, it is straightforward to integrate the total intensity over the image to obtain the total flux from the surface of the star. What remains is to specify the intensity as a function of direction and position on the surface. For simplicity, here the radiation is assumed to be a blackbody, which means that

the intensity is isotropic, and the distribution is specified by a single parameter, the temperature. § 5 outlines some of the complications of using a more complicated model for the emission.

As Heyl (2004) assumed, the temperature is proportional to a uniform component plus a component proportional to the local amplitude of the r-mode,

$$T(\theta, \phi) = T_0 \left\{ 1 + \frac{A}{2} \exp\left(\frac{3}{4} - \frac{1}{2}\eta^2\right) \left(\frac{1}{2} + \eta^2\right) \exp[i\phi - i(\Omega - \omega)t] \right\} \quad (7)$$

where $\eta = \cos\theta\sqrt{q/3}$ and $\Omega = 2\pi f$. The results of Heyl (2004) and Longuet-Higgins (1968) have been normalized and specialized for an r-mode with $q \gg 1$ and $m = \nu = 1$.

The specific intensity is taken to be given by the blackbody formula (e.g Shu 1991)

$$I_\nu = B_\nu(T) = \frac{2h\nu^3}{c^2} \frac{1}{e^{h\nu/kT} - 1} \quad (8)$$

and the total intensity is given by

$$\int I_\nu d\nu = \frac{2\pi^5}{15} \frac{k^4}{c^2 h^3} T^4. \quad (9)$$

Here only the temperature and frequency dependences are important, because the calculation is only concerned with relative variations in the flux not its absolute value.

An examination of Eqs. 7-9 shows how the waveform may develop higher harmonics. If the r-mode were taken to perturb the intensity directly, there would be no harmonics. Because the total observed flux would in this case be simply a weighed integral of the intensities over the surface of the star, the varying portion of the flux would be proportional to $\exp[-i(\Omega - \omega)t]$.

In the case considered here, the r-mode perturbs the temperature, so harmonics are naturally produced. The arguments from the preceding paragraph indicate the fundamental is simply proportional to A and only three higher harmonics are present in the total flux which are proportional to A^2 , A^3 and A^4 respectively. To lowest order in A , the pulsed fraction is proportional to A , so the ratio of the higher harmonics to the fundamental decreases rapidly as the pulsed fraction decreases. Because the specific intensity is a more complicated function of temperature (Eq. 8), when one looks at the variation at a specific energy, additional harmonics are generated, but each successive harmonic is weaker by a factor of A . This should be contrasted with the presence of a hot region (e.g. Munro et al. 2002). In the latter case, the ratio of the higher harmonics to the fundamental is set by the shape of the hot region and is independent of the amplitude of the temperature perturbation.

4. Results

To examine a wide range of physical effects and geometries, a large number of light curves were calculated. To appreciate how the various physical effects affect the light curves, some sample

light curves will be presented. A detailed discussion of how the light curves change as a function of energy, inclination, spin frequency, stellar compactness and the properties of the r-mode itself follows.

The effects of the varying redshift on the surface of the star, the time delay from different regions on the surface, and the inclusion of the perturbation of the exterior spacetime of the star due to rotation will be largest for star with the smallest radius and fastest spin rate viewed from near the equatorial plane. Fig. 1 depicts the light curves for a neutron star with $f = 1200$ Hz, $R/M = 3.87$ and an inclination of 5.739° .

The largest correction is obviously the varying redshift across the stellar surface. The varying redshift moves the peak of the emission earlier in phase, increases the pulsed fraction, and adds harmonics to the shape of the pulse. If one neglects frame dragging or varying time delay to different parts, the difference are much more modest. The frame dragging simply delays the phase of the decrease in the emission by a few degrees. The phase of the upswing is delayed by a slightly smaller amount. The time delay delays the phase of the decrease by about 15 degrees and delays the upswing by a slightly larger amount. Because only phase differences are observable, the main consequence of the time delay and the frame dragging is a very modest change in the shape of the light curves.

4.1. Energy Dependence

The properties of the burst oscillations depend strongly on energy as found by Muno et al. (2003). Specifically, the pulsed fraction increases dramatically with the energy of the radiation. Because the pulsed fraction is essentially proportional to the strength of the first harmonic, and the ratio of two consecutive harmonics scales with strength of the first harmonic. The harmonic content increases dramatically with increasing photon energy as shown in Fig. 2. Because the emission was assumed to have a blackbody spectrum, the flux from the surface of the star for $h\nu \gg kT$ is extremely sensitive to changes in the temperature on the surface. For emission well above the thermal peak, the pulsed fraction approaches unity and the higher harmonics become nearly as important as the fundamental.

The Doppler boosting of radiation originating from the half of the star approaching the observer causes the total flux from the surface to peak before the hot region crosses the line of the sight to the observer (see Fig. 1). As for the pulsed fraction, a slight increase in the ratio between the observed frequency and emitted frequency of photons in the Wein tail of the thermal radiation spectrum can have a dramatic effect on the observed flux, so higher energy radiation leads the emission at lower energies as shown in Fig. 3 (Ford 1999, 2000).

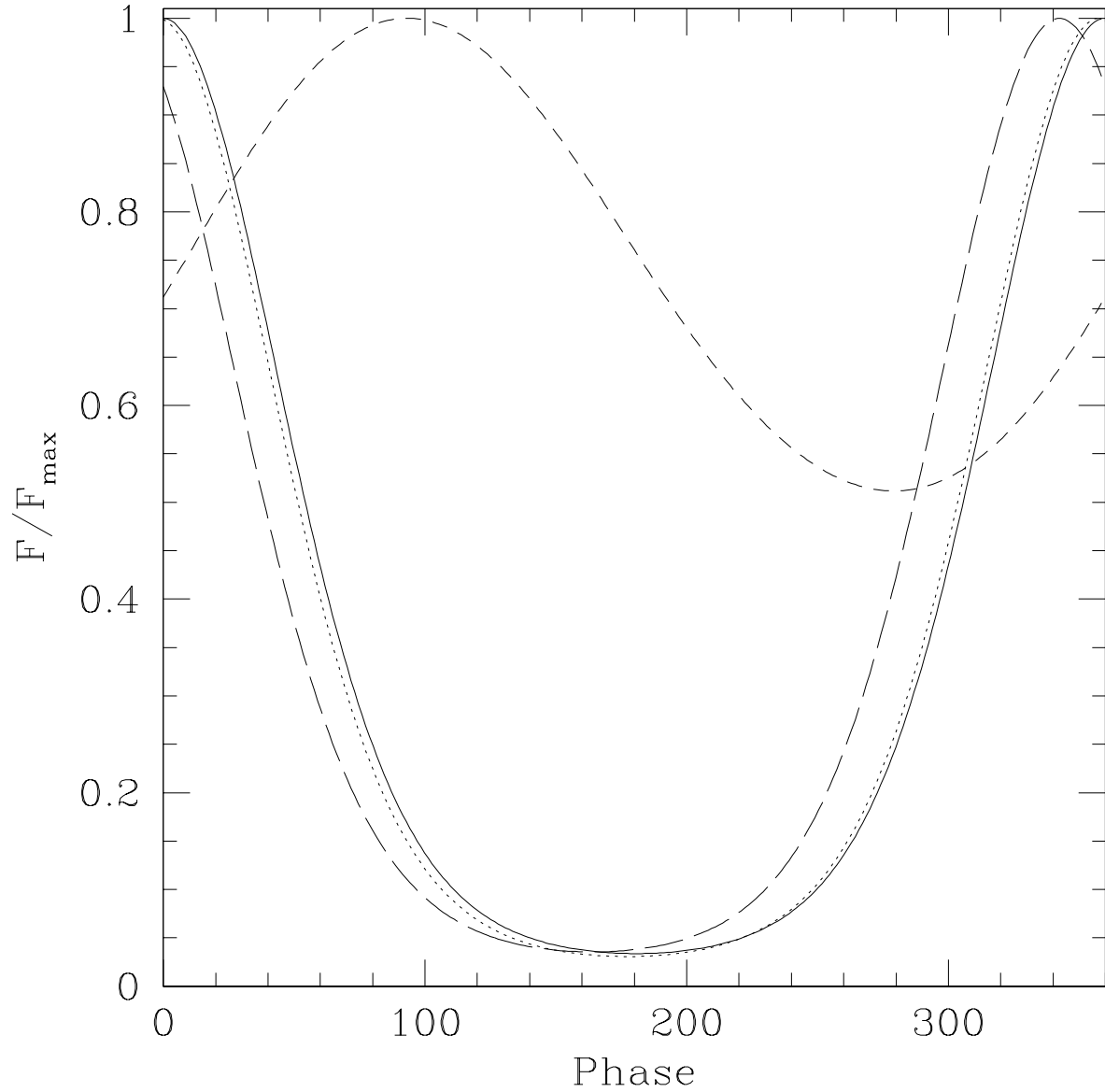


Fig. 1.— The light curves for a rapidly rotating neutron star with various physical effects neglected. The solid curve gives the light curve with all relativistic effects included. The dotted curve neglects the perturbation to the spacetime induced by the spin of the star. The long-dashed curve neglects the time delay from various parts of the surface, and the short-dashed curve neglects the variation in the redshift across the surface of the star. $f = 1200$ Hz, $R/M = 3.87$, $i = 5.739^\circ$, $A = 0.05$ and $q = 100$.

Table 1. Parameter Values

Parameter	Definition	Values
M	Mass of star	$1.4 M_{\odot}$
f	Spin frequency of star	0, 300, 600, 1200 Hz
i	Latitude of line of sight	$5.739^{\circ}, 17.46^{\circ}, 30^{\circ}, 44.43^{\circ}, 64.18^{\circ}$
$\sin i$	Cumulative solid angle	0.1, 0.3, 0.5, 0.7, 0.9
R	Stellar radius	8, 10, 12, 14 km
$Rc^2/(GM)$	Stellar compactness	3.87, 4.84, 5.80, 6.77
$h\nu/kT_0^a$	Dimensionless photon energy	0.3, 1, 3, 10, 30
A	R-mode amplitude	0.05, 0.15, 0.5
$q \equiv 2\pi f/\omega$	Spin-mode frequency ratio	100, 300, 600, 1200

^aThis is the unpulsed emiss

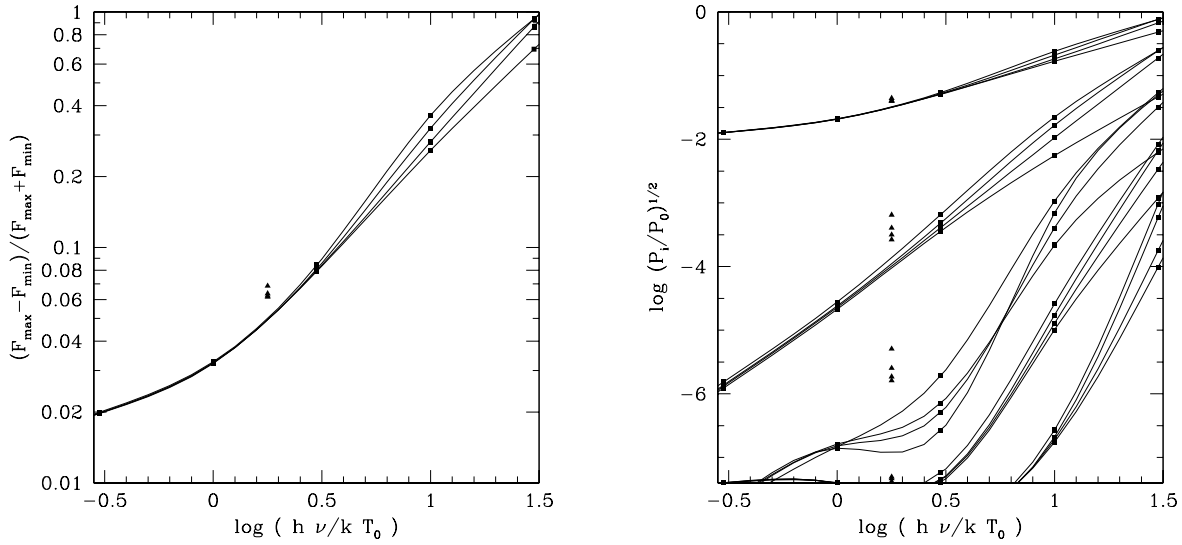


Fig. 2.— The pulsed fraction and harmonic content as a function of energy. In the left panel, the curves from bottom to top are for stellar spin frequencies $f = 0, 300, 600$ and 1200 Hz. The triangular symbols give the result for the total flux. In the right panel, each bundle of four curves traces the power in a successive harmonic, starting at the top with the first harmonic. Within each bundle the four curves traces the same stellar spin frequencies as in the left panel. The other parameters are held constant at $i = 30^{\circ}$, $R/M = 4.84$, $A = 0.05$ and $q = 100$

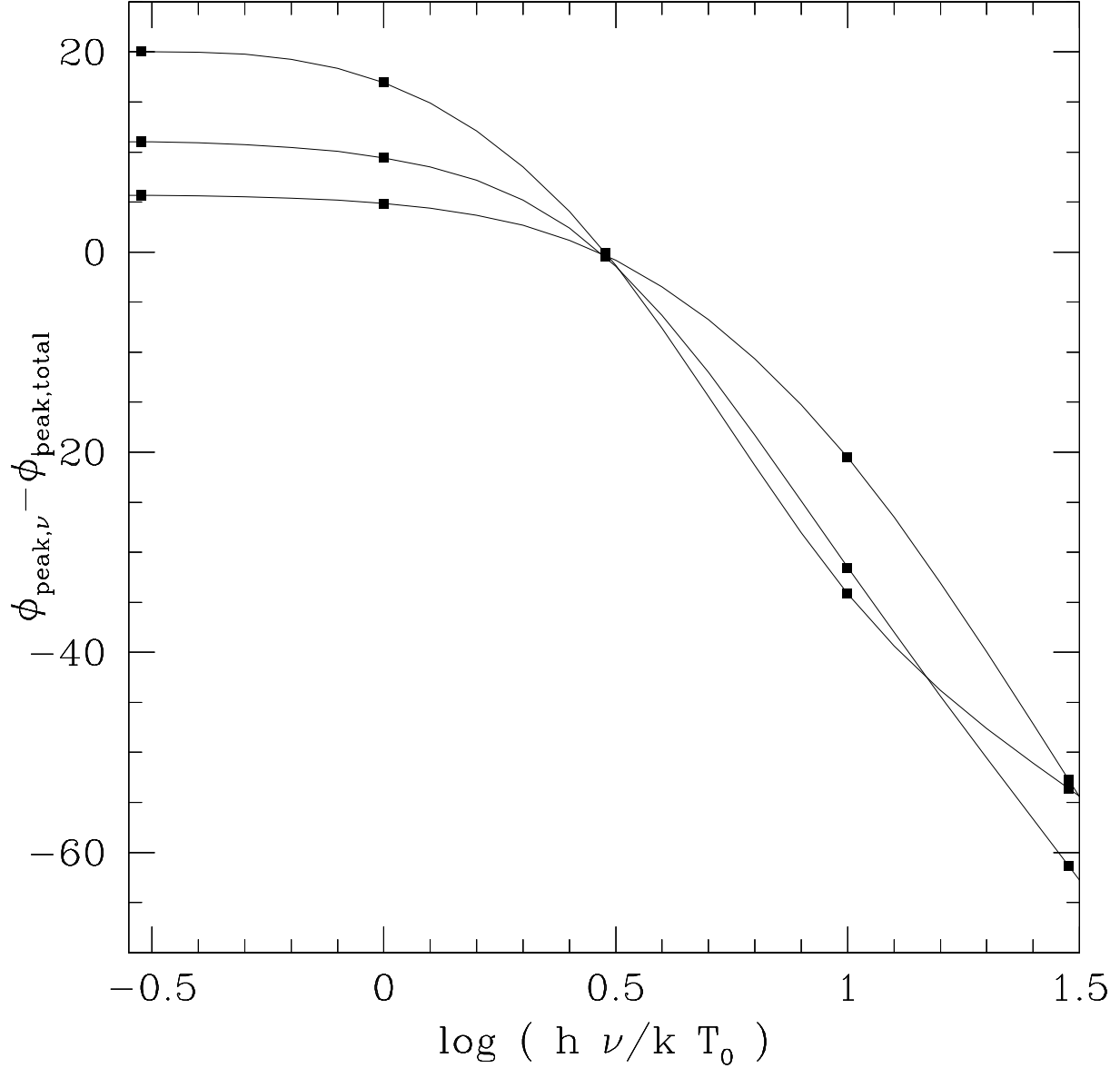


Fig. 3.— Phase lag as a function of photon energy and stellar spin. The curves depict the phase lag of the peak at a particular energy of the emission relative to peak of the total flux. The peak at low energies comes after the peak of the total flux, while the peak at high energies leads the total flux. The largest absolute values of the lag/lead are for the fastest spinning stars. The curves trace $f = 300, 600$ and 1200 Hz and the other parameters are at $i = 30^\circ$, $R/M = 4.84$, $A = 0.05$ and $q = 100$

4.2. Inclination and Compactness

The observed light curves of course depend on the inclination of equator of the star relative to our line of sight and the compactness of the star, R/M . Because the hot region lies along the equator of the star, the pulse fraction and harmonic content depend only weakly on the inclination of the spin axis of the star (Fig. 4). Of course, the pulse fraction and harmonic content vanish for $i = 90^\circ$, but for inclinations up to 64.18° , i.e. over 90% of the lines of sight, the pulse fraction is nearly constant.

As is well known (Page & Sarmiento 1996) more compact stars typically exhibit less variability because the gravity bends null trajectories from the rear of the star to reach the observers; therefore, an equatorial hot region may be visible during an entire rotation of the star. Fig. 5 bears this out for the r-mode oscillations. The r-modes are uniquely sensitive to the physically interesting compactness while being relatively insensitive to the inclination of the star (*c.f.* the results of Weinberg et al. 2001; Muno et al. 2002, for hot spots). This makes them a potentially important probe of the equation of state of neutron stars.

4.3. R-mode properties

To examine how the properties of the r-mode affect the resulting light curves, both the value of $q = 2\pi f/\omega$ and the amplitude of the r-mode (A) are varied. As Heyl (2004) noted as q varies both the size of the r-mode on the surface of the star changes and the observed frequency of the oscillation $f(1 - 1/q)$. Here the focus will be the former effect exclusively.

The end of § 3 argues that the ratio of the i harmonic to the $(i + 1)$ harmonic is simply A . Fig. 7 demonstrates that this is indeed the case even as a function of the photon energy. This result contrasts with the results for a hot spot that exhibits a constant ratio between the strengths of the various harmonics. This effect is a robust prediction of the r-mode model for Type-I X-ray burst oscillations.

5. Discussion

The paper examines the properties of the variability in the flux from the surfaces of neutron stars from Type-I X-ray burst oscillations. Because the underlying emission is known and fixed by the detection of the oscillations themselves, r-modes provide a unique and powerful tool to understand the properties of the underlying neutron star. This situation must be contrasted with hot spot models (*e.g.* Muno et al. 2002) in which the size, position and number of hot spots are *a priori* unknown and the observed lightcurves depend sensitively on these properties.

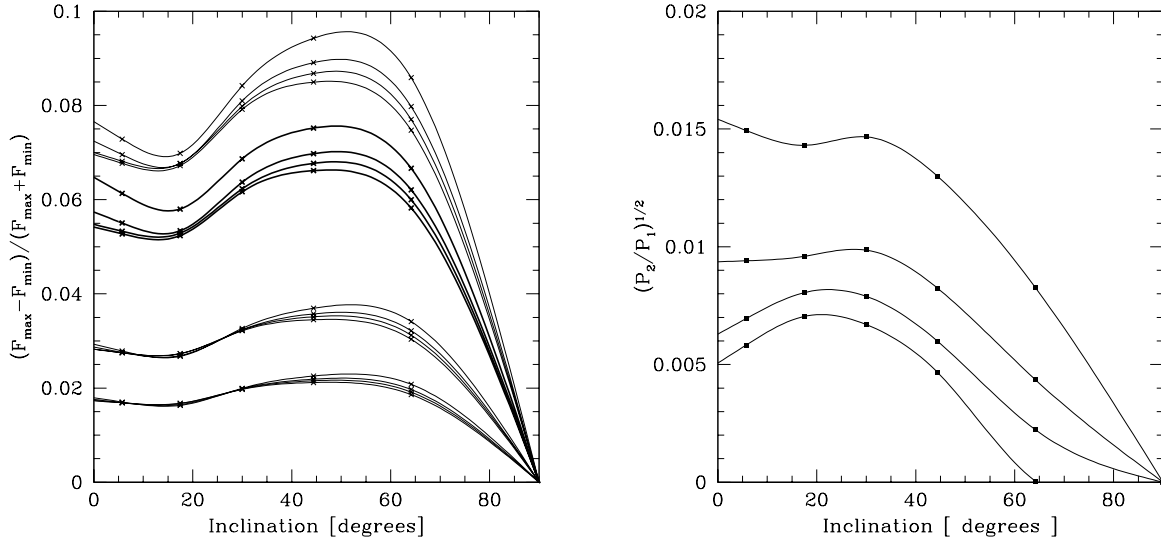


Fig. 4.— The pulsed fraction and harmonic content as a function of inclination. The the left panel each bundle of four curves depicts the results for a different photon energy. From top to bottom they are $h\nu/kT_0 = 3$, the total flux (bold) and $h\nu/kT_0 = 1$ and 0.3 . Within each bundle are the results for different spins, $f = 0, 300, 600$ and 1200 Hz from bottom to top. The right panel depicts the ratio of the power of the total flux in the second harmonic to that in the first harmonic. From bottom to top are depicted the different stellar spins of $f = 0, 300, 600$ and 1200 Hz. The other parameters are fixed at $R/M = 4.84$, $A = 0.05$ and $q = 100$

Muno et al. (2002) found that the amplitude of the fundamental oscillation during the tail of the x-ray bursts typically was five to ten percent. They only obtained upper limits to the strength of the higher harmonics that were less than a tenth of that of the fundamental. These results agree quite nicely with the results presented in this paper. This low harmonic content is difficult to account for in a hot spot model (see Fig. 3–8 of Muno et al. 2002).

This paper argues that the pulsed fraction should increase dramatically with increasing photon energy. Muno et al. (2003) found just this trend in the burst oscillations. However, Muno et al. (2003) found that the peak in the emission at high energies lags that at lower energies. This contradicts the theoretical models presented here as well as those of Muno et al. (2003) and Ford (1999). Muno et al. (2003) argue that the high-energy photons may be generated through Compton scattering of lower energy photons in the accretion disk corona (*e.g.* Miller 1995). A similar conclusion must be drawn in the context of this model, reducing its utility to understand the observed oscillations at the highest energies.

6. Conclusion

R-modes on the surface of neutron stars during Type-I X-ray bursts present a rich phenomenology and may provide a useful new method to determine the parameters of neutron stars such as their masses and radii. When one observes a Type-I X-ray burst oscillation, several of the parameters listed in Tab. 1 can be obtained easily – f , the spin frequency of the star and q , the ratio of the spin frequency to the frequency of the mode. The remaining parameters, including the mass and radius of the star can be determined from observations of the pulsed fraction and harmonic content as a function of energy.

Only two parameters describe the r-mode excitation on the surface of the star – q that is determined by measuring the frequency drift of the burst oscillation (Heyl 2004) and A by calculating the ratio of the first harmonic to the fundamental frequency of the oscillation observed at a particular frequency (*e.g.* Fig. 7). With the properties of the surface pattern fixed, the pulsed fraction and phase lag as a function of energy can determine the remaining physical parameters, R and M . The pulse fraction is not particularly sensitive to the geometric parameter i . Burst oscillations may be a powerful probe of both the physics of nuclear burning on the surfaces of neutron stars and of the nuclear equation of state. To realize the full potential of these techniques requires relativistic calculations of both the interior of rotating neutron stars and ray tracing through the external spacetime as well as atmospheric modelling.

Support for this work was provided by the National Aeronautics and Space Administration through Chandra Postdoctoral Fellowship Award Number PF0-10015 issued by the Chandra X-ray Observatory Center, which is operated by the Smithsonian Astrophysical Observatory for and on behalf of NASA under contract NAS8-39073.

REFERENCES

- Cadeau, C., Leahy, D. A., & Morsink, S. M. 2005, *ApJ*, 618, 451
- Chen, K. & Shaham, J. 1989, *ApJ*, 339, 279
- Ford, E. C. 1999, *ApJ*, 519, L73
- . 2000, *ApJ*, 535, L119
- Heyl, J. S. 2004, *ApJ*, 600, 939
- Longuet-Higgins, M. S. 1968, *Phil. Trans. R. Soc.*, 262, 511, (LH68)
- Miller, M. C. 1995, *ApJ*, 441, 770
- Muno, M. P., Özel, F., & Chakrabarty, D. 2002, *ApJ*, 581, 550
- . 2003, *ApJ*, 595, 1066
- Page, D. & Sarmiento, A. 1996, *ApJ*, 473, 1067
- Ravenhall, D. G. & Pethick, C. J. 1994, *ApJ*, 424, 846
- Shu, F. H. 1991, *The Physics of Astrophysics: Volume I. Radiation* (Mill Valley, California: University Science Books)
- Stergioulas, N. & Friedman, J. L. 1995, *ApJ*, 444, 306
- Weinberg, N., Miller, M. C., & Lamb, D. Q. 2001, *ApJ*, 546, 1098

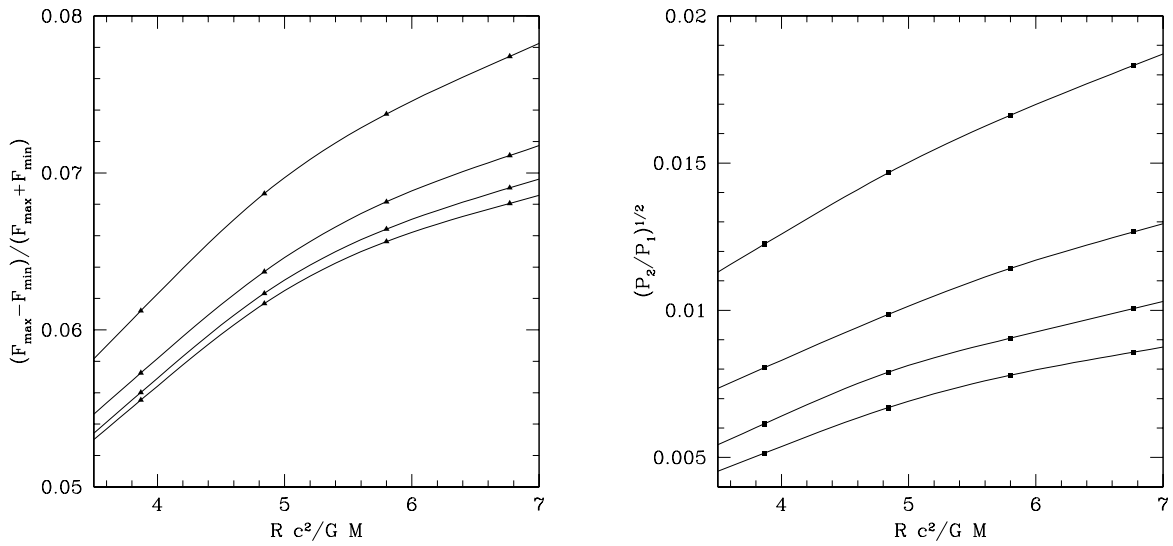


Fig. 5.— The pulsed fraction and harmonic content as a function of radius. The left panel depicts the total pulsed fraction as a function of stellar radius and spin. The right panel depicts the ratio of the power of the total flux in the second harmonic to that in the first harmonic. From bottom to top in panel the curves are the different values of stellar spin, $f = 0, 300, 600$ and 1200 Hz. The other parameters are fixed at $i = 30^\circ$, $A = 0.05$ and $q = 100$

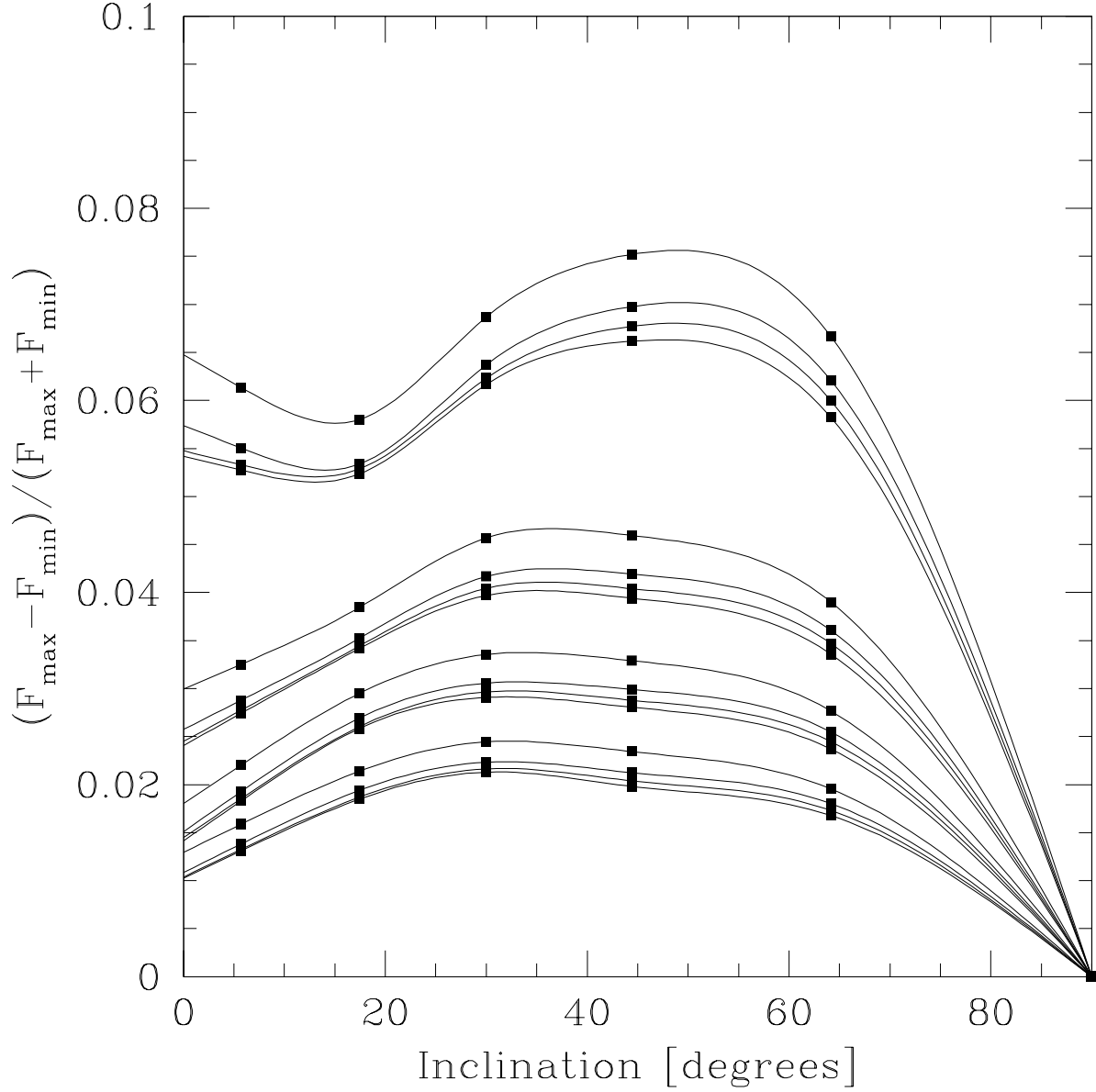


Fig. 6.— Pulsed fraction as a function of q . The curve depicts the total pulsed fraction as a function of inclination, q and f . The bundles of curves are from top to bottom are for $q = 100, 300, 600$ and 1200 . Within each bundle are the stellar spins from bottom to top of $f = 0, 300, 600$ and 1200 Hz.

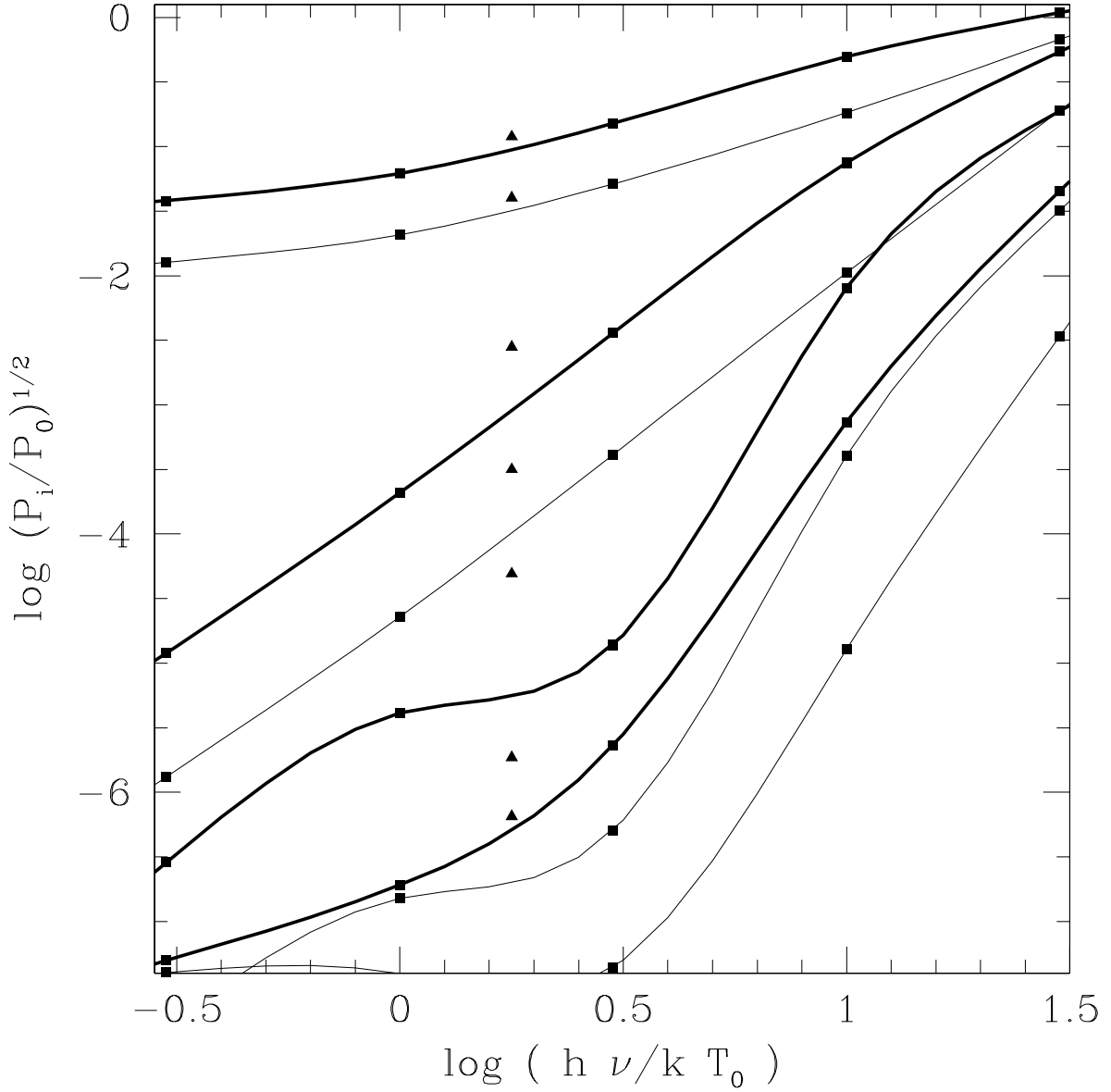


Fig. 7.— Harmonic content as a function of A . The bold curves have $A = 0.15$ and the light curves have $A = 0.05$. The triangles give the result for the total flux, and the curves trace the ratio of the flux in the first, second, third and fourth harmonics from top to bottom. The other parameters are $i = 30^\circ$, $R = 4.84M = 10 \text{ km}$, $q = 100$ and $f = 300 \text{ Hz}$.